Supporting Information

Energy-level engineering of the electron transporting layer for improving open-circuit voltage in dye and perovskite-based solar cells

Seong Sik Shin[1], Jae Ho Seok[2], Bong Joo Kang[3], Wenping Yin[4], Seon Joo Lee[1], Jun Hong Noh[5], Tae Kyu Ahn[6], Fabian Rotermund[3], In Sun Cho[8,*] and Sang Il Seok[1,8,*]

1. Division of Advanced Materials, Korea Research Institute of Chemical Technology, 141 Gajeong-Ro, Yuseong-Gu, Daejeon 34114, Republic of Korea

2. Department of Materials Science and Engineering, Seoul National University, Seoul, 151-744, Republic of Korea

3. Department of Physics, Korea Advanced Institute of Science and Technology (KAIST), 291, Daehak-ro, Yuseong-gu, Daejeon, 34141, South Korea

4. Materials Science and Engineering, Monash University & ARC Centre of Excellence in Exciton Science (ACEx)

5. School of Civil, Environmental and Architectural Engineering, Korea University, 145 Anam-ro, Seongbuk-gu, Seoul 02841, Republic of Korea

6. Department of Energy Science, Sungkyunkwan University, 2066 Seobu-ro, Jangan-gu, Suwon 16419, Korea.

7. Department of Materials Science & Engineering and Energy Systems Research, Ajou University, 206 Worldcup-ro, Yeongtong-gu, Suwon, Gyeonggi-do 16499, South Korea

8. School of Energy and Chemical Engineering, Ulsan National Institute of Science and Technology, 50 UNIST-gil, Eonyang-eup, Ulju-gun, Ulsan 44919, Republic of Korea.

*Corresponding Authors: insuncho@ajou.ac.kr; seoksi@unist.ac.kr

Methods

Synthesis of $Ba_{1-x}Sr_xSnO_3$ NPs.

All chemicals for the preparation of NPs were of reagent grade and were used without further purification. 2.467 g of $BaCl_2 \cdot 2\,H_2O$ (99 %, Aldrich) and 3.577 g of $SnCl_4 \cdot 5\,H_2O$ (98 %, Aldrich) were dissolved in hydrogen peroxide aqueous solution (170 mL; 30 %, OCI) using constant stirring. To replace Ba with Sr ($Ba_{1-x}Sr_xSnO_3$), $Sr(NO_3)_2$ (99 %, Aldrich) was introduced depending on X. To suppress agglomeration of particles, 0.961 g of citric acid was added to mixed solution. The pH of the reaction solution was adjusted to a value of 10 using ammonia solution (25 %, OCI). With addition of ammonia solution, the transparent solution turns milky white and gradually become pure white due to precipitation of precursors. To obtain crystalline precipitate, the reaction mixture was held at 40^{o}C in water bath for the 12 h whilst continually stirring. According to laboratory environment, temperature and time can be changed from 40 to 60^{o}C and 1 to 12 h, respectively. In fact, the crystalline precipitate is formed within 1h. After a reaction time of 12 h, the white precipitate was thoroughly washed with distilled water and absolute ethanol, the product was obtained by centrifugation. The obtained products were then dispersed in 2-methoxy ethanol with using ultrasonicator. Before depositing BSO precursor film, the colloidal solution was filtered with 0.45 μm PVDF membrane filter.

Solar Cell Fabrication.

A F-doped SnO_2 (FTO, Pilkington, TEC8) substrates were chemically etched with zinc powder and dilute HCl solution, and cleaned by sonication in deionized water, acetone, and ethanol. A

dense blocking layer of TiO_2 (bl-TiO_2, ~70nm in thickness) was deposited onto a F-doped SnO2 (FTO, Pilkington, TEC8) substrate by spray pyrolysis, using a 20 mM titanium diisopropoxide bis(acetylacetonate) solution (Aldrich) at 450°C to prevent direct contact between the FTO and the hole-conducting layer. For PSCs, a BSO thin film was prepared by spin coating the colloidal dispersion of BSO particles onto Bl-TiO_2-coated FTO glass at 3,000 r.p.m. for 30 s, followed by calcining on a hot plate at 500°C for 1 h. To control film thickness, the procedure was repeated several times. For depositing perovskite layers, all processes were performed at low humidity condition (~15% RH). CH_3NH_3I (MAI) was first synthesized by reacting 27.86 mL CH_3NH_2 (40% in methanol, Junsei Chemical) and 30 mL HI (57 wt% in water, Aldrich) in a 250 mL round-bottom flask at 0°C for 4 h with stirring, respectively. The precipitate was recovered by evaporation at 55°C for 1 h. MAI were dissolved in ethanol, recrystallized from diethyl ether, and dried at 60°C in a vacuum oven for 24 h. The prepared MAI powder and PbI_2 (99.9985 %, Alfa aesar) for 0.8 M $MAPbI_3$ solution were stirred in a mixture of 2-Methoxyethanol, Dimethly sulfoxide (DMSO) (99.9%, Aldrich) and gamm-Butyrolactone (GBL) (99%, Aldrich) (7:3:4 v/v) at 50°C for 10 min. The resultant solution was deposited onto the prepared BSO film by a consecutive two-step spin coating process at 1,000 and 5,000 r.p.m. for 10 and 20 s, respectively, at 20% RH and 25°C. During the second spin coating step, the film was treated with toluene drop-casting, and then was dried on a hot plate at 100°C for 10 min. For depositing hole transporting materials, a solution of poly(triarylamine) (EM index, Mn=17,500 g mol^{-1}, 15 mg in toluene 1.5 ml) was mixed with 15 μl of a solution of lithium bistrifluoromethanesulphonimidate (170 mg) in acetonitrile (1 ml) and 7.5 μl 4-tert-butylpyridine. The resulting solution was spin coated on the $CH_3NH_3PbI_3$/BSO based-thin film at 3,000 r.p.m. for 30 s. Finally, an Au counter electrode was deposited by thermal evaporation.

For DSSCs, mesoscopic BSO films were prepared on FTO glass substrates from a homemade paste including BSO nanoparticles via a screen-printing method. To control film thickness, the procedure was repeated several times. The coated films were annealed under an ambient atmosphere following multiple heating steps (325°C for 5 min, 375°C for 5 min, 450°C for 15 min, and then 500°C for 15 min). For the $TiCl_4$ treatment, the annealed BSO films were immersed in a 0.05 M $TiCl_4$ aqueous solution for 3 min at 50°C. Then, the films were sintered again at 500°C for 30 min. For the dye adsorption, the BSO films were soaked in a dye solution (0.5 mM purified N719 dye in absolute ethanol) at room temperatures for 60 min. In this case, the soaking time for the BSO films is much shorter than that for conventional materials (e.g., 20 h for TiO_2) due to the fast dye adsorption kinetics on the BSO surface. After the dye adsorption process, the films were thoroughly rinsed with a mild stream of absolute ethanol to remove the physically adsorbed dye molecules. For liquid DSSCs, Sandwich-type DSSCs were then assembled using the dye-adsorbed BSO film and a platinized FTO substrate (by sputtering) with a hot-melt film (~60 μm, Surlyn) between them. Finally, an iodide-based liquid electrolyte (SI16 L1535-01, Merck) was infiltrated into the cell through a hole from the counter electrode side. For solid state DSSCs, the hole transporting layer was deposited by spin coating 0.15 M Spiro-OMeTAD (dissolved in chlorobenzene) solution including 0.12 M tBP, 0.2 M Li-TFSI (predissolved in acetonitrile) and cobalt complex for 30 s at 2000 rpm. Finally, an Au counterelectrode was deposited by thermal evaporation.

Characterization.

The crystal structure and phase of the materials were characterized using an XRD (New D8 Advance, Bruker). The morphologies and microstructures were investigated by field emission

scanning electron microscopy (FESEM, SU 70, Hitachi) and transmission electron microscopy (JEM 3000F, JEOL). The optical properties of samples were characterized using an ultraviolet–visible spectrophotometer (UV 2,550, Shimadzu). X-ray photoelectron spectroscopy (XPS) studies were carried out using a Thermo VG Scientific K-Alpha. The EQE was measured using a power source (300W xenon lamp, 66,920, Newport) with a monochromator (Cornerstone 260, Newport) and a multimeter (Keithley 2001). The electrochemical measurement for Mott-Schottky analysis was conducted at the frequency of 1 kHz with a 1 M KCl aqueous solution (pH 7). The J–V curves were measured using a solar simulator (Oriel Class A, 91,195A, Newport) with a source meter (Keithley 2,420) at 100mWcm-2, AM 1.5 G illumination, and a calibrated Si-reference cell certified by the NREL. The J–V curves were measured by reverse scan (forward bias (1.2 V) - short circuit (0 V)) or forward scan (short circuit (0 V) - forward bias (1.2 V)). The step voltage and the delay time were fixed at 10mV and 40ms, respectively. The J–V curves for all devices were measured by masking the active area with a metal mask 0.096 cm^2 in area. Time-dependent current and dark current, impedance and capaciatance voltage measurments were measured with a potentiostat (PGSTAT302N, Autolab) under one sun illumination. Impedance measurement was carried out at DC bias of V = 0.1 V under 1 sun illumination with the frequency ranging between 1 MHz and 0.01 Hz. Capacitance voltage (CV) measurements were performed at fixed frequency (1 kHz), employing the ITO/$_{Ba1-x}Sr_xSnO_3$/perovskite/Au heterojunction structured devices. All measuremts were performed at room temperature.

An electrochemical workstation (Zennium, Zahner) with an attached frequency response analyzer and a lightemitting diode (667 nm) was utilized for the intensity-modulated photovoltage spectroscopy study. Transient photovoltage decay measurements were performed using a nanosecond laser (10 Hz, NT342A-10, EKSPLA) as a small perturbation light source and a Xe lamp (150 W, Zolix) as a bias light source. The device was directly connected to a

digital oscilloscope (500 MHz, DSO-X 3054A, Agilent) and the input impedance of the oscilloscope was set to 1 MΩ for an open circuit condition. The bias light intensity was controlled by neutral density filters for various open circuit voltages (V_{OC}) and a strongly attenuated laser pulse of 550 nm, which generated a voltage transient (ΔV) that did not exceed 20 mV.

Table S1. Crystal structures of synthesized $Ba_{1-x}Sr_xSnO_3$ solid solution ($0 \leq x \leq 0.5$)

Material	Crystal system	Lattice parameters	Unit cell Volume
$BaSnO_3$	Cubic	a=4.117715 b=4.117715 c=4.117715	69.81823
$Ba_{0.95}Sr_{0.05}SnO_3$	Cubic	a=4.115379 b=4.115379 c=4.115379	69.69948
$Ba_{0.9}Sr_{0.1}SnO_3$	Cubic	a=4.111382 b=4.111382 c=4.111382	69.49659
$Ba_{0.8}Sr_{0.2}SnO_3$	Cubic	a=4.105271 b=4.105271 c=4.105271	69.18716
$Ba_{0.7}Sr_{0.3}SnO_3$	Cubic	a=4.102051 b=4.102051 c=4.102051	69.02448
$Ba_{0.5}Sr_{0.5}SnO_3$	Tetragonal	a=5.780385 b=5.780385 c=8.151023	272.3489

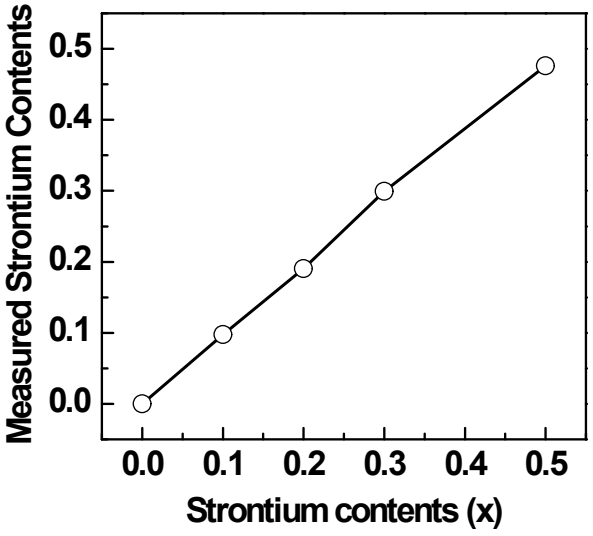

Fig. S1 ICP-MS analysis of synthesized $Ba_{1-x}Sr_xSnO_3$ solid solution ($0 \leq x \leq 0.5$).

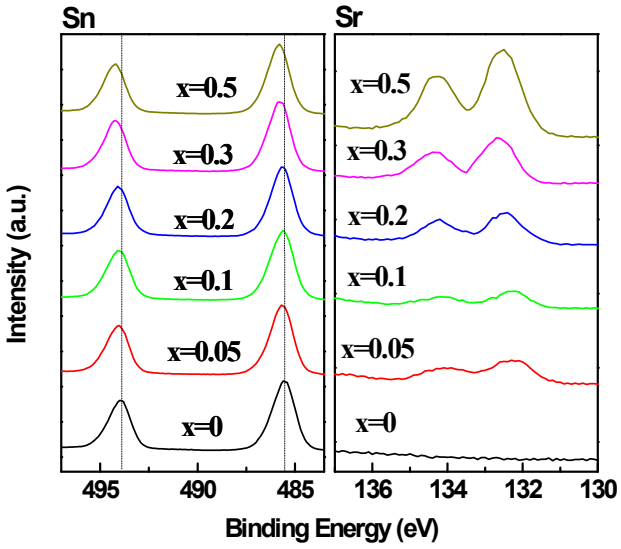

Fig. S2 XPS spectra of synthesized $Ba_{1-x}Sr_xSnO_3$ solid solutions ($0 \leq x \leq 0.5$).

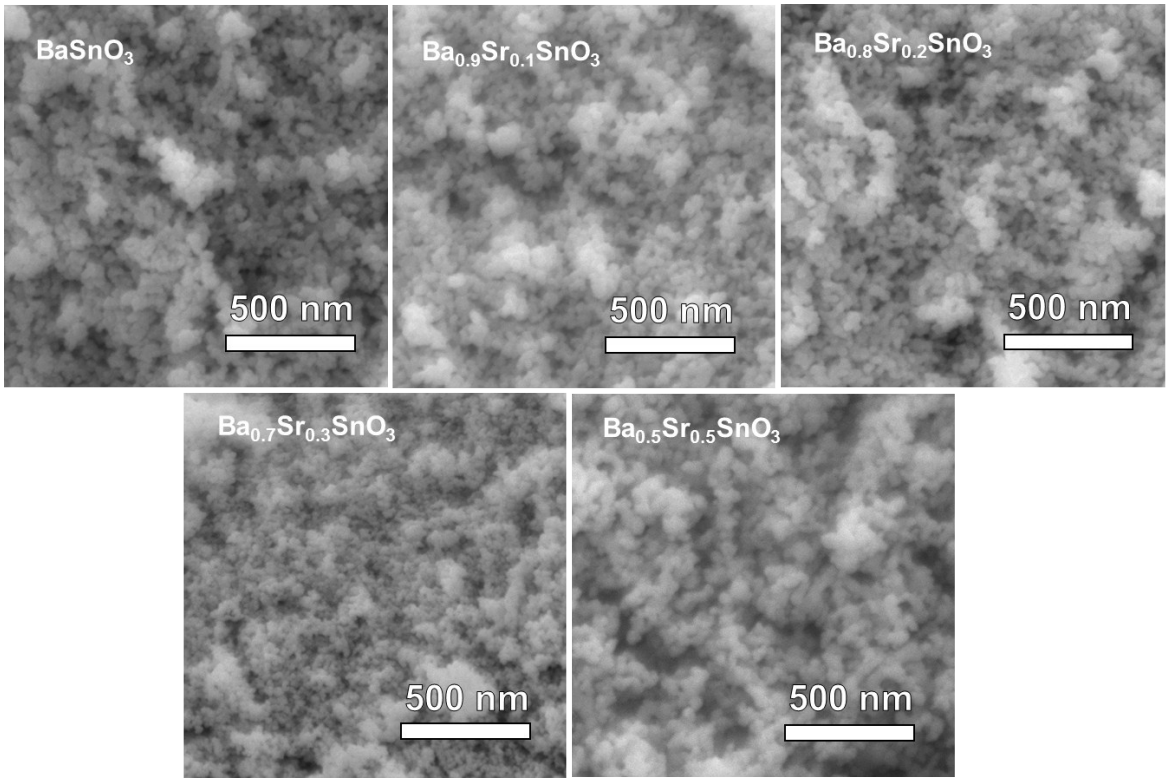

Fig. S3 SEM images of synthesized $Ba_{1-x}Sr_xSnO_3$ ($0 \leq x \leq 0.5$) powders.

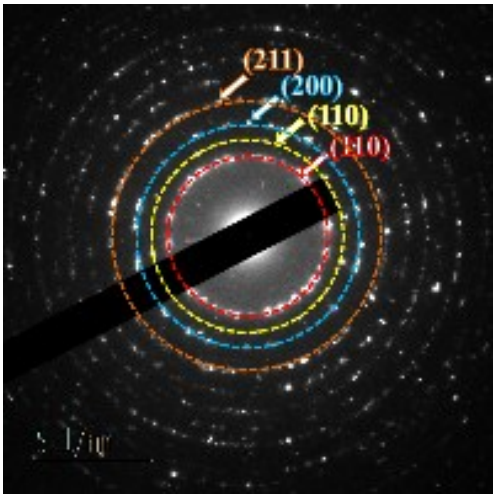

Fig. S4 SAED pattern of the synthesized $Ba_{0.8}Sr_{0.2}SnO_3$ NPs.

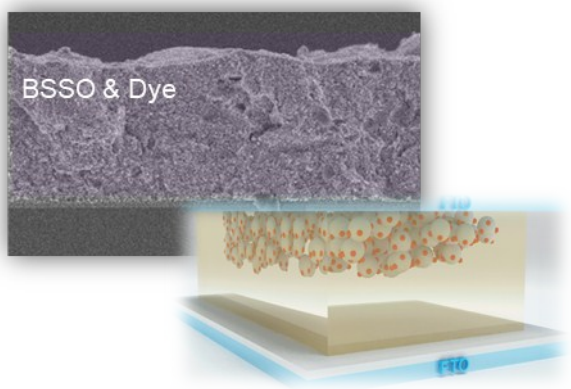

Fig. S5 Architecture for dye-sensitized solar cell using $Ba_{1-x}Sr_xSnO_3$ NPs as electron transporting layer.

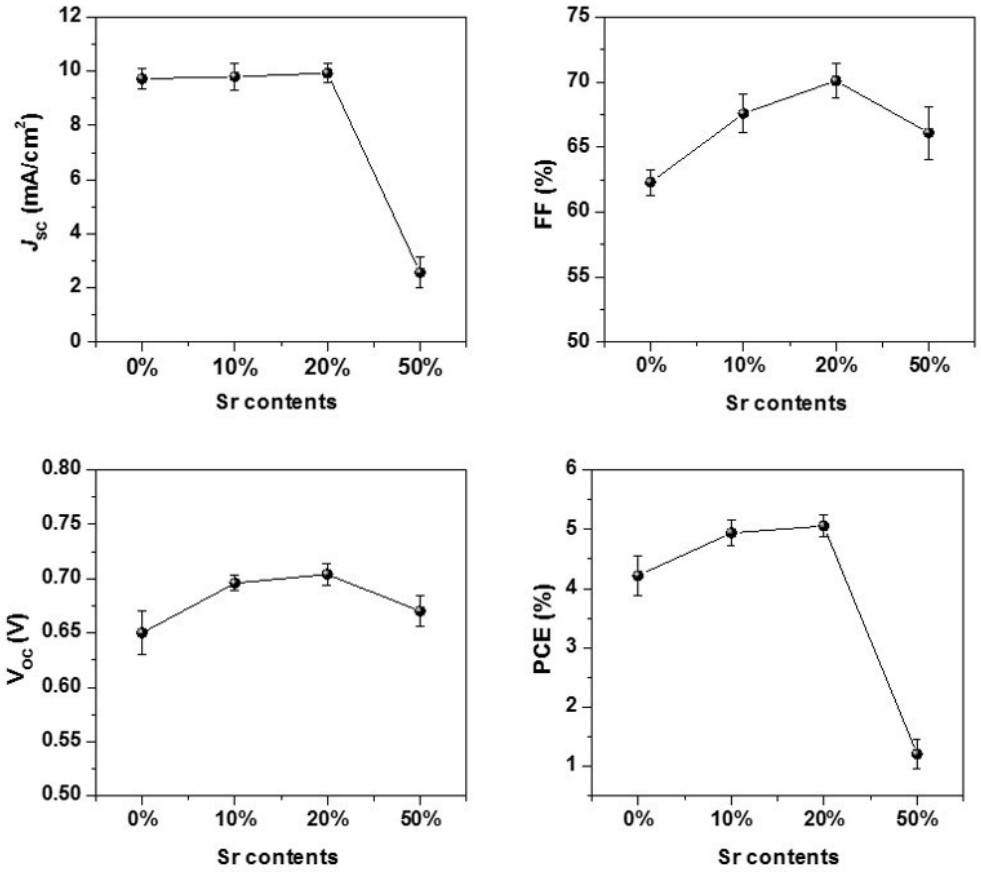

Fig. S6 Statistics of PCEs extracted from *J-V* curves for $Ba_{1-x}Sr_xSnO_3$ ($0 \leq x \leq 0.5$) based DSSCs

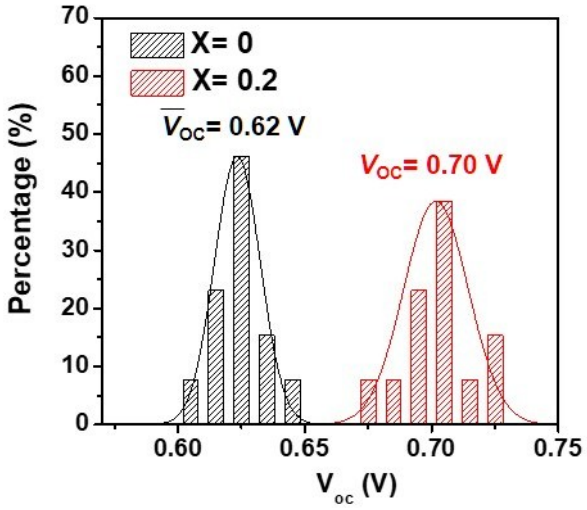

Fig. S7 Distribution of V_{oc} extracted from *J-V* curves of DSSCs fabricated with $BaSnO_3$ and $Ba_{0.8}Sr_{0.2}SnO_3$.

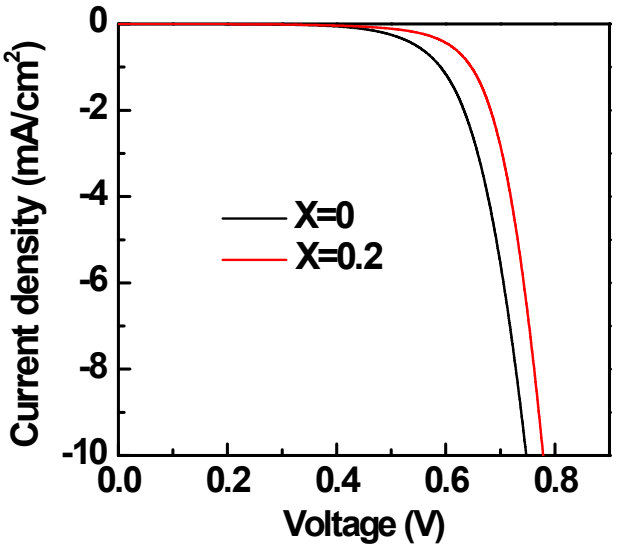

Fig. S8 Dark *J-V* curves for $BaSnO_3$ and $Ba_{0.8}Sr_{0.2}SnO_3$ based DSSCs.

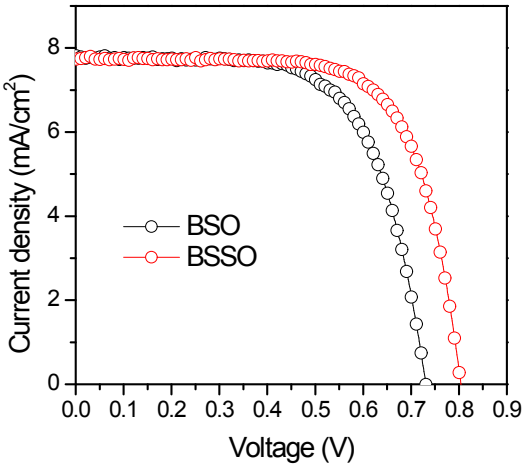

Fig. S9 Comparison of *J-V* curves of DSSCs fabricated with $BaSnO_3$ and $Ba_{0.8}Sr_{0.2}SnO_3$ using solid-state hole conductor (Spiro-OMeTAD)

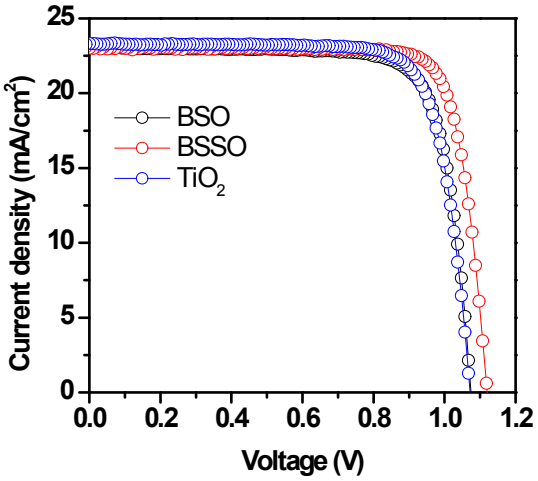

Fig. S10 Comparison of *J-V* curves of PSCs fabricated with $BaSnO_3$, $Ba_{0.8}Sr_{0.2}SnO_3$ and TiO_2. TiO_2 based PSC shows similar device performance to $BaSnO_3$ based PSC.

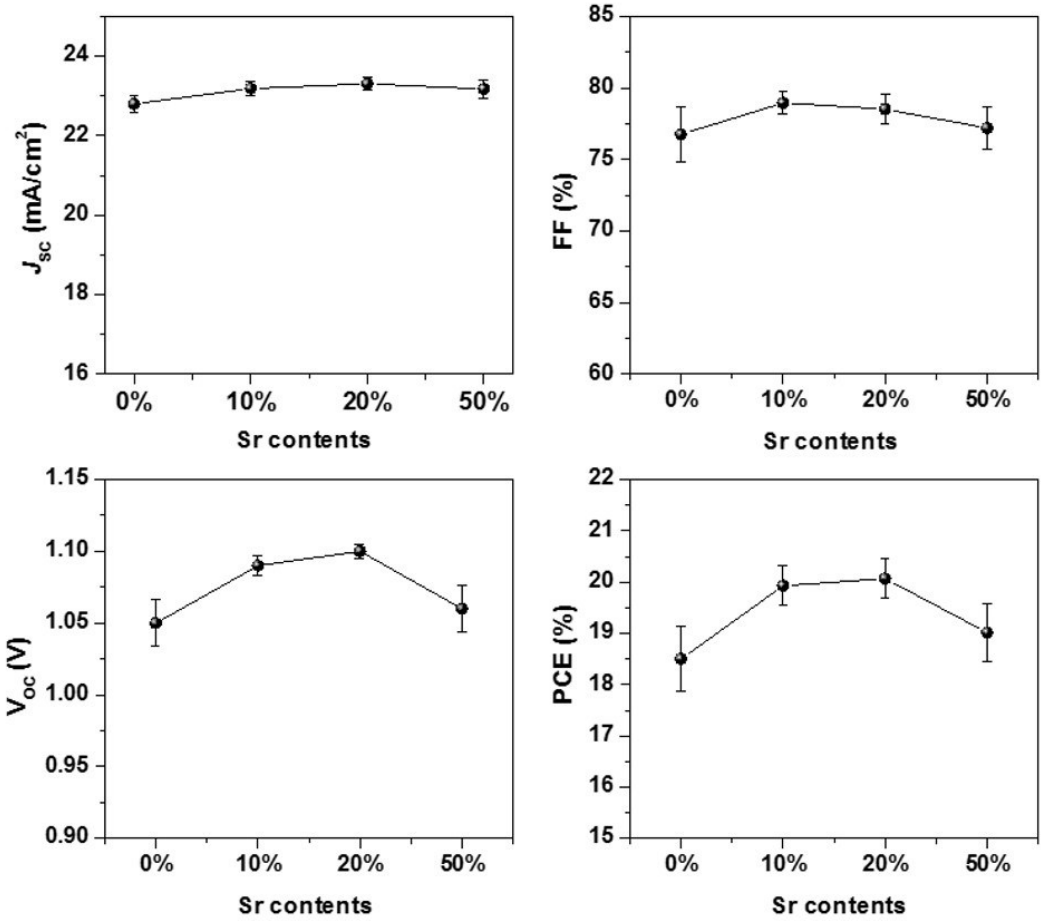

Fig. S11 Statistics of PCEs extracted from *J-V* curves for $Ba_{1-x}Sr_xSnO_3$ ($0 \leq x \leq 0.5$) based PSCs

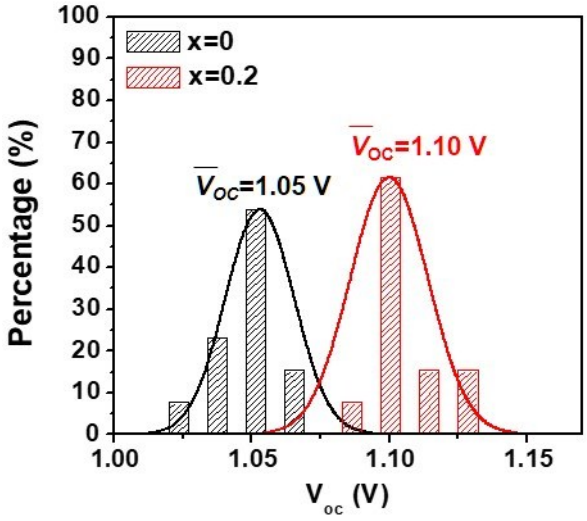

Fig. S12 Distribution of V_{OC} extracted from *J-V* curves of PSCs fabricated with $BaSnO_3$ and $Ba_{0.8}Sr_{0.2}SnO_3$.

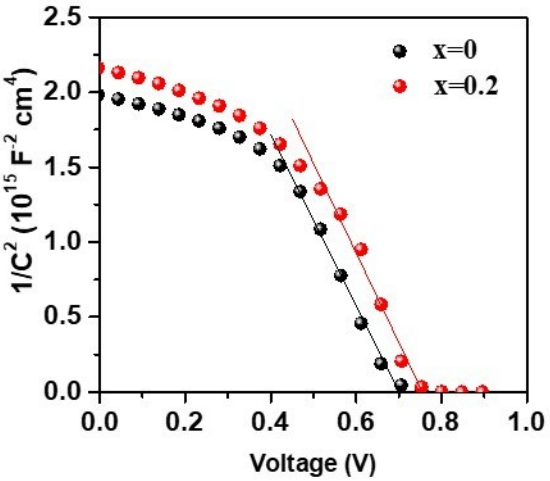

Fig. S13. Mott-Schottky measured between perovskite and ETLs with different x in $Ba_{1-x}Sr_xSnO_3$.

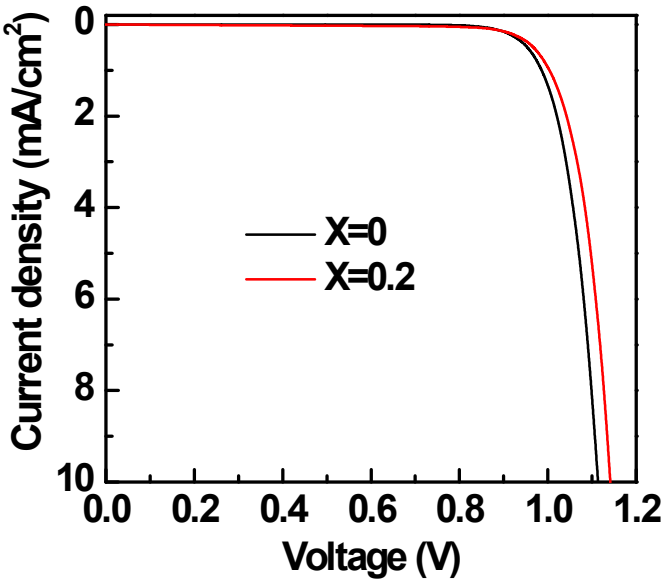

Fig. S14. Dark *J-V* curves for $BaSnO_3$ and $Ba_{0.8}Sr_{0.2}SnO_3$ based PSCs.

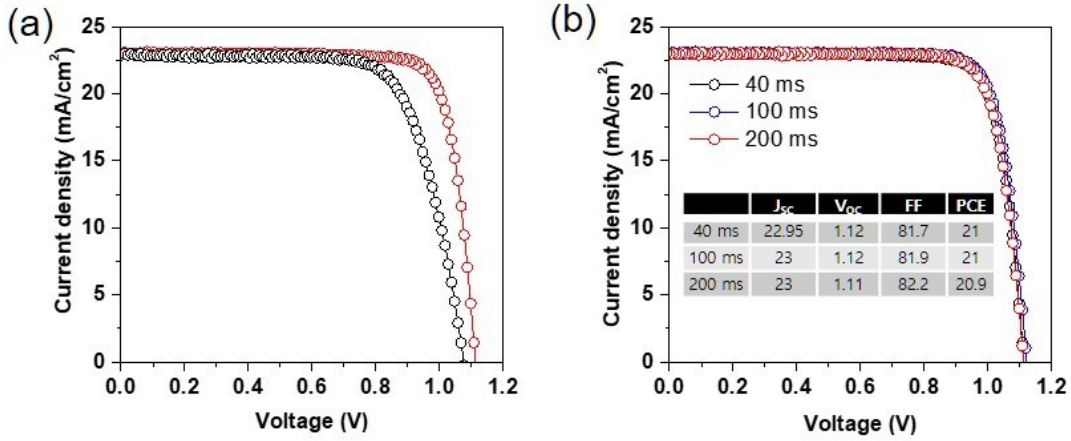

Fig. S15. *J-V* curves of the best-performing device, based on $Ba_{0.8}Sr_{0.2}SnO_3$, measured with reverse (red color) and forward (black color) scans, and a different delay time.

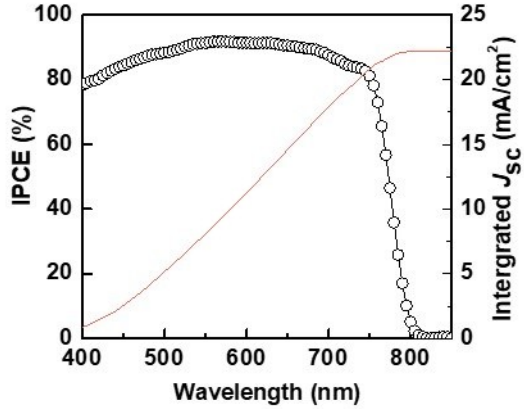

Fig. S16. IPCE of best-performing device fabricated with $Ba_{0.8}Sr_{0.2}SnO_3$ as ETL.

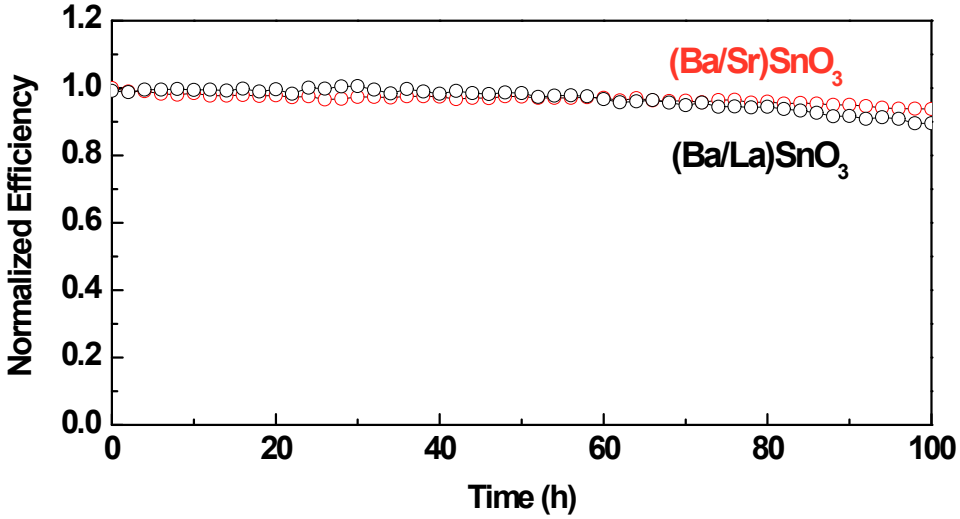

Fig. S17. Photostability for BSSO and LBSO-based PSCs.